

ERS-ENVISAT Permanent Scatterers Interferometry

C. Colesanti¹, A. Ferretti², C. Prati¹, D. Perissin¹, F. Rocca¹

¹ Dipartimento di Elettronica e Informazione, Politecnico di Milano, Piazza L. da Vinci, 32 -20133 Milano, Italy, Phone: +39-02-23993697, Fax: +39-02-23993413, E-mail: colesant@elet.polimi.it

² Tele-Rilevamento Europa - T.R.E. S.r.l., Via V. Colonna, 7 -20149 Milano, Italy

Abstract – The Permanent Scatterers (PS) technique [1], [2], [3], is a powerful and fully operational tool for monitoring ground deformations on a high spatial density grid of point-wise targets, exploiting long series of SAR data. The most attractive aspect of this approach is the capability of providing measurements relative to individual radar targets with unprecedented precision. Up to now, PS analyses have been carried out on ERS, RADARSAT, and JERS data sets. The purpose of this presentation is to discuss the feasibility of updating results obtained by means of a PS analysis on ERS interferometric data using ENVISAT ASAR images. In particular, the main goal is to stitch coherently the new ENVISAT ASAR measurements to the already available ERS displacement time series relative to individual PS. To this end, we will model the interferometric phase of point-wise targets taking account the different ERS and ENVISAT carrier frequencies. Then, we identify the main constraints to be met at individual Permanent Scatterers in order to guarantee the feasibility of coherent stitching.

I. ERS AND ENVISAT: AUTO- AND CROSS-INTERFEROGRAMS

Besides several important technological improvements, the key difference between ERS and ENVISAT is the 30 MHz central frequency change from 5.3 to 5.33 GHz. This change entails advantages as well as disadvantages: classical interferometry on distributed scatterers is made impossible, unless the normal baseline ranges from –1000 m to –3000 m [4], [5], [6] so that the wavenumber shift ensures sufficient range common band.

Thus, high baseline cross-interferograms¹ can be generated and very high precision DEM estimation becomes possible. A very interesting application could be the topographic characterization of flood plains. However, volumetric decorrelation effects are likely to be very strong and, therefore, extremely short revisiting times would be important to guarantee at least a negligible temporal decorrelation. To this end it should be kept in mind that ERS-2 operates now in Zero Gyro Mode and, therefore, looking for short temporal baseline pairs, constraints for ERS-

ENVISAT cross-interferometry on distributed scatterers are set on the Doppler Centroid value as well.

Since, of course, these rather strict requirements are not systematically met, two different strategies can be considered for continuing the phase histories of individual scatterers.

In the case of point scatterers (or at least scatterers with a reduced slant range extension) the baseline range allowing for a prediction of the phase signature from the ERS to the ENVISAT operating frequency is extended and cross-interferograms can be created without strict constraints on the normal baseline. In fact point scatterers are imaged coherently with both systems by definition. Their phase histories can be stitched moving from one to the other frequency. Of course this requires the correction of the deterministic phase terms depending on the scatterer position coupled with the normal baseline and the frequency shift (the expression is provided in the next paragraph).

Alternatively, we can consider classical auto-interferograms only and bridge the frequency change in a similar way to what is carried out in Small Baseline Interferometry [7]. This can be performed by combining the two distinct interferogram classes (namely ERS-ERS and ENVISAT-ENVISAT) basing on a model adopted for motion (the interferogram classes can be temporally intertwined, as long as ERS-2 operations are continued).

Two main advantages of using cross-interferograms are:

- The possibility of long term interferometry from 1991 to the end of the life of ENVISAT, allowing one to measure very slow earth motions on a pixel by pixel basis in a unique **coherent** time series (all data are referred to a single master acquisition);
- The possibility of **determining with high precision the location of the scatterer**, exploiting the slant range dependent phase shift in cross-interferograms.

In fact, the phase shift due to the change of frequency from f_0 to $f_0 + \Delta f$, for a given PS with slant range position and elevation respectively Δr and Δq (both relative to the center of the sampling cell taken as origin of the coordinates) is:

$$\Delta\phi = \frac{4\pi}{c} \left\{ \Delta r \Delta f + \Delta r \frac{f_0 B_n}{r_M \tan \theta} + \Delta q \frac{f_0 B_n}{r_M \sin \theta} \right\}$$

¹ With cross-interferograms we refer to interferograms between ERS and ENVISAT images.

where c is the light speed, B_n the normal baseline, r_M the sensor-target distance and θ the incidence angle.

Besides the flat Earth and topography phase terms a new contribution depending on the frequency shift and on the slant range position of the point wise target arises. Given the 30 MHz frequency variation, the phase change across a slant range resolution cell amounts to about 4π . Therefore, (besides the exact elevation) the location of the scatterer within the cell has to be known with about 1m precision, to be able to predict its phase within one radian. On each ERS-ENVISAT cross-interferogram a Location Phase Screen (LPS) will be superimposed (in correspondence of the PS). The LPS is uncorrelated in space but is the same in all cross-interferograms since both the PS slant range position and the frequency shift are constant. As a matter of fact the LPS values in the cross-interferograms at PS will yield the PS positions within the resolution cell.

Interestingly, we can note that for usual single frequency PS interferograms, a similar LPS is created by the occurrence of an earthquake. Due to aliasing, the sudden change in the position of all PS with respect to the previous acquisitions, corresponds to a spatially uncorrelated LPS. In absence of relevant post-seismic deformation the PS positions are then constant. The continuation of the PS phase histories bridging an earthquake, is therefore conceptually similar to the continuation of the PS time series coping with a constant carrier frequency variation.

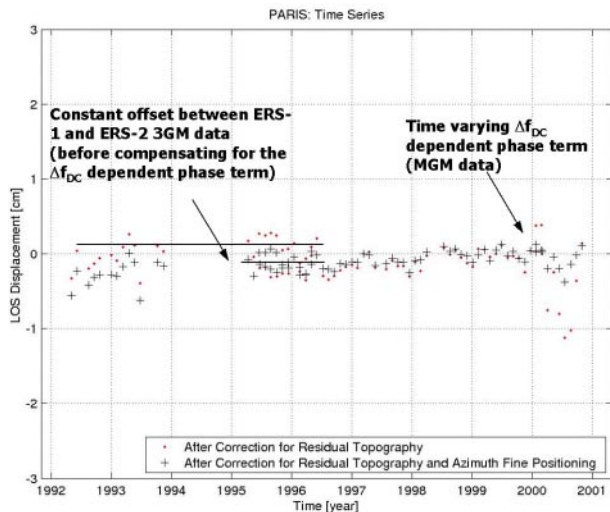


Figure 1: Displacement time series of a single PS before (red) and after (black) compensating the phase term depending on the sub-cell azimuth PS position coupled with varying (MGM since Feb. 2000) Doppler Centroids. Analogous results have been obtained also involving ZGM ERS-2 data.

This is, in turn, a simplified version of the problem faced in order to cope with a Doppler Centroid change, that translates in an additional phase term depending on the scatterer

location along azimuth (with respect to the center of the sampling cell). Of course, in this case, the Doppler Centroid difference is approximately constant between ERS-1 and ERS-2 3-Gyro-Mode (3GM) data but is highly variable in successive Mono- and Zero-Gyro-Mode (MGM and ZGM) acquisitions (Figure 1).

II. AMPLITUDES OF ERS VS ENVISAT

A first simple analysis can be carried out comparing ERS and ENVISAT average amplitude values at individual ERS PS (single pixel multi-image coherence >0.8 [1], [2], [3]) after registering the ENVISAT images available on the ERS sampling grid (test site: Milano, 90 ERS images, 3 ENVISAT images (two of which acquired during the commissioning phase)). A cross-plot is depicted in Figure 2.

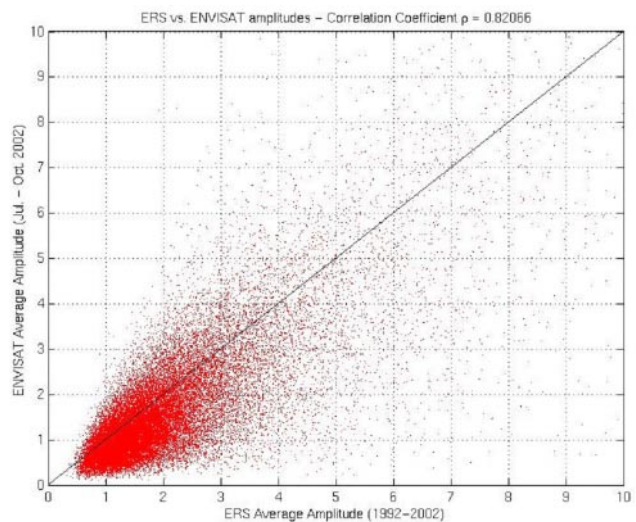


Figure 2: ERS vs. ENVISAT average amplitudes at ERS PS.

From the amplitude ratio A_{ENVI}/A_{ERS} , the cross range size ρ of PS can be estimated assuming a flat scattering surface (scattering distributed on part of the sampling cell) and attributing the amplitude loss to the directivity².

$$\rho = \frac{r_M \lambda}{\pi B_n} \cdot \sqrt{\frac{3}{2} \left(1 - \frac{A_{ENVI}}{A_{ERS}} \right)}$$

The histogram represented in Figure 3 has been obtained for (considering the PS that are “better pointed” towards ERS (i.e. resonate better at the ERS frequency)).

² The less effective resonance of partially distributed ERS PS at the ENVISAT carrier frequency is modeled using the duality normal baseline – frequency shift [4].

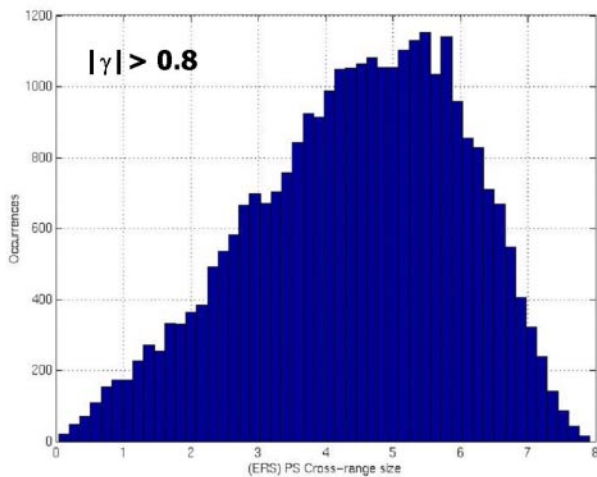


Figure 3: Cross range size of ERS PS estimated from the amplitude variation from ERS to ENVISAT data

III. ERS PS IN ENVISAT INTERFEROGRAMS

A further preliminary experiment that deserves being carried out is the investigation of the behavior of ERS PS in ENVISAT interferograms. Generating ENVISAT-ENVISAT interferograms (after resampling the images on the ERS grid), and exploiting the results of a PS analysis carried out on ERS data, it was possible to compensate the ENVISAT interferometric phases at ERS PS for topography and ground deformation phase terms. Finally, working at a scale of a few km², the atmospheric disturbances (as well as baseline errors) can be reduced strongly fitting and removing from the (wrapped) phase residuals a plane with a limited dynamic range. The histogram of the phase residuals at ERS PS in an ENVISAT interferogram (20021015-20020806) clearly show that excellent ERS PS (coherence ≥ 0.95) behave as very good PS (coherence ~ 0.91) in ENVISAT interferograms as well (Figure 4).

IV. CONCLUSIONS

We have discussed briefly the framework we are using to continue coherently ERS PS time series with ENVISAT data exploiting cross-interferograms at privileged small radar targets. Both requirement and by product (at once) is sub-cell PS positioning along slant range. Finally, we have shown the very first results obtained comparing ERS and ENVISAT amplitudes as well as analyzing the ENVISAT phase behavior at ERS PS.

ACKNOWLEDGMENTS

The authors are very thankful to ESA for the ENVISAT and ERS data (provided under ESRIN contract No. 16564/02/I-LG) as well as to the whole T.R.E. staff.

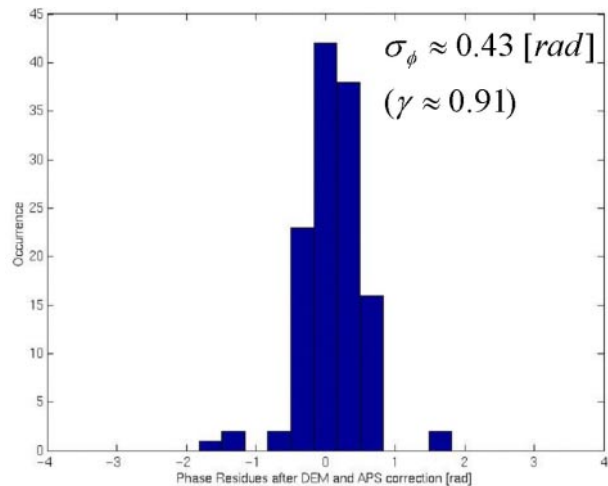


Figure 4: Phase residuals (at ERS PS) in an ENVISAT interferogram, a first experimental evidence that very good ERS PS behave as PS for ENVISAT as well.

REFERENCES

- [1] A. Ferretti, C. Prati, F. Rocca, "Permanent Scatterers in SAR Interferometry", IEEE TGARS, Vol. 39, no. 1, 2001.
- [2] A. Ferretti, C. Prati, F. Rocca, "Non-linear subsidence rate estimation using permanent scatterers in Differential SAR Interferometry", IEEE TGARS, Vol. 38, no. 5, 2000.
- [3] C. Colesanti, A. Ferretti, C. Prati, F. Rocca, "Monitoring Landslides and Tectonic Motion with the Permanent Scatterers Technique", Eng. Geology, Vol. 68/1-2, 2003.
- [4] F. Gatelli et al., "The Wavenumber Shift in SAR Interferometry", IEEE TGARS, Vol. 32, no. 4, 1994.
- [5] N. Adam, "Das erste Cross-Interferogramm aus Aufnahmen der Radarsensoren ENVISAT/ASAR und ERS-2", available on-line at: http://www.caf.dlr.de/caf/aktuelles/archiv/bilderarchiv/envisat/cross_interferogramm/_cross_interferogramm
- [6] A. Monti Guarnieri, C. Prati, "ERS-ENVISAT Combination for Interferometry and Super-resolution", ERS-ENVISAT Symposium (Gothenburg, Sweden), 1222 October, 2000.
- [7] P. Berardino, G. Fornaro, R. Lanari, E. Sansosti, "A new algorithm for surface deformation monitoring based on small baseline differential SAR interferograms", IEEE TGARS, Vol. 40 no. 11, 2002